Bioceramics Development and Applications

Salem et al., Bioceram Dev Appl 2017, 7:1
DOI: 10.4172/2090-5025.1000100

Research Article Open Access

Electrical Transport Properties and Gamma-Ray Attenuation Coefficient of Some Phosphate Glasses Containing By-Pass Cement Dust

Salem SM, Mostafa AG, Ahmed MA, Yassin OM and Abu Gasser RA*

Department of Physics, Faculty of Science, Al-Azhar University, Nasr City, Cairo, Egypt

Abstract

Some phosphate glasses containing different amounts of by-pass cement dust (BCD) were prepared by the melt quenching method. The selected molecular composition was [(100-x)% - P_2O_5 (x)% BCD (where 30≤ x≥60)]. The obtained experimental density and molar volume values were inspected and were then compared with those obtained empirically for the close packed structure of the corresponding compounds. The comparison between experimental and emperical values evidenced the short range order of the studied samples. The electric and dielectric properties were thoroughly investigated. The appearance of maxima and minima in the total conductivity BCD concentration dependence can be attributed to the mixed alkali – alkaline earth effect (MAAE) and to the presence of considerable amount of CaO. The suitability of such glasses to act as gamma-ray shielding materials was thoroughly investigated, and correlation between the chemical composition (the BCD concentration) and gamma-ray attenuation behavior was established.

Keywords: By-pass cement dust; Phosphate glasses; Electrical transport properties; Gamma – ray attenuation

Introduction

Amorphous materials and glasses appear now of interest due to their important functional applications in both science and technology [1]. Therefore, much efforts have been devoted to study either high purity glasses samples used for scientific purposes, or others doped with a controlled amount of impurities used for commercial application [2,3]. Among all scientific applications, electrical transport properties are of interest, where some glasses can be used as electrically insulators while some others can be used as conductors depending mainly on their compositions. It is known also that the amount and type of the introduced alkali oxide into a glass network affect directly relation with several properties of such glass [4-6]. Therefore, the understanding of the electrical conductivity of glasses is very important. Although a great deal of work has been done to determine the electrical conductivity in such like glasses, more work is still needed to clarify the true mechanism of conduction [5-7].

From another point of view the use of different radioactive isotopes now in industry, medicine, agriculture etc, make it necessary to study various materials that possess shielding character. For different nuclear radiation, special shielding materials are required [8-10].

From another point of view, by-bass cement dust (BCD) represents a dangerous by-product of cement industry and it accumulated in huge amounts in Egypt. It causes various diseases, especially those related to human respiratory system [11]. According to the chemical analysis, such waste consists of various oxides (mainly, CaO, SiO_2, Na_2O, K_2O and Fe_2O_3) [12,13], where all these oxides can be used for manufacturing different types of oxide glass [13].

However, in this article, it will be tried to prepare some phosphate glasses with different additives of BCD, as high as possible, aiming to consume the waste accumulation as well as to obtain low coast glasses that can be used for different industrial and scientific application. Also, the prepared glasses will be thoroughly investigated from the electrical properties point of view as well as their gamma-ray shielding properties, in order to obtain some shielding transparent glasses as well as, they can act to capsulate the radio-active wastes before interment underground.

Experimental Procedure

BCD was supplied by Tora Cement Co., Helwan, Cairo, Egypt, and it was chemically analyzed using X-ray fluorescence technique (model, Panalytical Axios advanced, The Netherlands). The obtained chemical analysis is exhibited in Table 1.

The selected glass batches were weighted from ammonium di-hydrogen ortho-phosphate and the supplied BCD, so that when melted, they give glasses having the following percentage molecular composition [(70-x) P_2O_5 - x BCD, where 30 ≤ X≥ 60 in steps of five]. The weighted batches were ground and mixed well in an agate mortar and they were then melted in porcelain crucibles in an electric muffle furnace for 2 hrs at 110°C. Melts were stirred several times during melting, and were then poured between two copper plates in the

Constituents	Cement dust
SiO_2	6.96
Al_2O_3	2.36
Fe_2O_3	3.60
CaO	60.36
MgO	1.54
Na_2O	0.03
K_2O	10.74
L.O.I.	16.59
Total	100
*L.O.I.= Loss of Ignition	

Table 1: The chemical composition of the used BCD.

***Corresponding author:** Gasser R, Department of Physics, Faculty of Science, Al-Azhar University, Nasr City, Cairo, Egypt, Tel: +20 102 722 7142; E-mail: drahmedgamal@yahoo.com

Received March 20, 2017; **Accepted** April 20, 2017; **Published** April 25, 2017

Citation: Salem SM, Mostafa AG, Ahmed MA, Yassin OM, Abu Gasser RA (2017) Electrical Transport Properties and Gamma-Ray Attenuation Coefficient of Some Phosphate Glasses Containing By-Pass Cement Dust. Bioceram Dev Appl 7: 100. doi: 10.4172/2090-5025.1000100

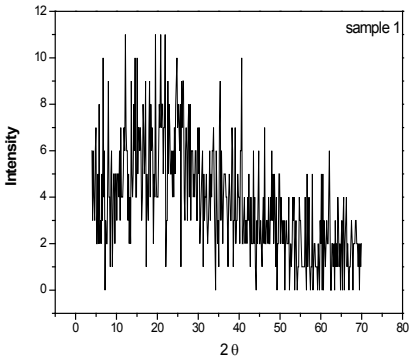

Figure 1a

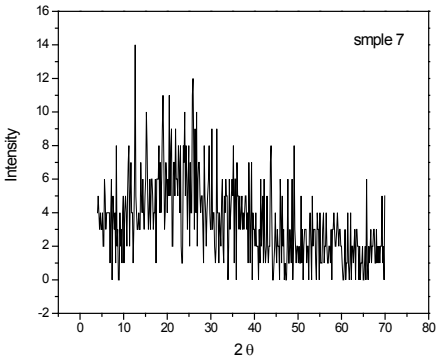

Figure 1b

Figure 1: (a and b) (XRD) of the samples containing 30 and mol% BCD.

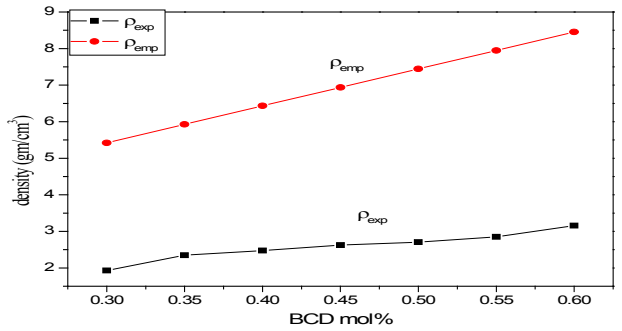

Figure 2: The variation of both density values (experimental and empirical) versus BCD content.

environmental air. The obtained glass samples, just after solidifying, were transferred to the annealing furnace at 450°C for 2 hrs and the furnace was then turned off and left to cool to RT with a cooling rate of 0.42 K/min.

The XRD spectra of the prepared samples were obtained using (Rigaku RINT2100) outfitted with (Cuk$_\alpha$ radiation of λ= 0.1541 nm) and the maximum current and voltage were 300 mA and 50 KV respectively.

The experimental density was measured applying Archimedes technique, using carbon tetra-chloride (CCl_4) as an immersion liquid, using equation (1),

$$\rho_{exp} = \left[\frac{M_a}{M_a - M_l}\right] \quad (1)$$

where ρ_{exp} and *Pl* are the experimental density of a sample as well as the density of the iquid respectively, M_a and M_l are the masses of the sample in air and in liquid respectively.

The experimental molar volume values (V_m) were then calculated using equations (2) [14].

$$(V_m)_{exp} = \frac{M_m}{\rho_{exp}} \quad (2)$$

where (M_m) is the main molecular weight in (g/mol) of a sample and ρ_{exp} is the experimental density value of such sample.

The empirical density values were also calculated using the following equation:

$$\rho_{emp} = \sum_i p_i x_i \quad (3)$$

where ρ_i are the densities of the oxides forming the glass and X_i is the mole fraction of each oxide.

The empirical molar volume values were then calculated using equation (3) but with replacing ρ_{exp} by ρ_{emp} [14].

For the electrical measurements, the obtained glasses were polished from both sides in order to obtain optically flat disk shape samples of 8 mm diameter and 2 mm thickness. Then the disks were coated from both sides with an air drying silver paste to achieve good electrical contact. The measurements were carried out using a computerized Stanford LCR bridge model SR 720 at four fixed frequencies [0.12 kHz, 1 kHz, 10 kHz and 100 kHz], and all measurements were performed in the temperature range from 300 K to 525K.

Results and Discussion

The amorphous nature of the prepared samples was examined visually where they all appeared transparent, homogenous and having no crakes or air bubbles.

For more conformation, X-Ray Diffraction (XRD) technique was applied to confirm the amorphous nature of the prepared samples. Therefore, Figures 1a and 1b shows the XRD patterns of the glasses containing 30 and 60 mol% BCD as representative patterns, and all other patterns show similar spectra.

These patterns show no any discreet lines or sharp peaks, but only a hump appeared at 2θ between 20° and 30° degree indicating that the prepared samples are all of amorphous nature and short range order character.

The density values of the studied glasses were experimentally measured applying the liquid displacement technique. The empirical values were also calculated applying equation (3) and the obtained values were compared with those obtained theoretically for the close packed structure of the corresponding compounds.

Both the experimental and empirical density values are exhibited in Figure 2 as a function of BCD content, for comparison. It is seen that both density values (empirical and experimental) increased gradually and linearly with the gradual increase of BCD, and the empirical density is usually higher than the corresponding experimental density values.

Since the molar volume is directly related to the internal spatial structure of materials, it is suitable to exhibit also the change of

the molar volume of the studied glasses [14]. Figure 3 exhibits the variation of the calculated molar volume values (both empirical and experimental) as the BCD was gradually increased, where it show a linear gradual decrease. It is observed also that the empirical values are usually lower than those obtained experimentally.

Also, the rate of the decrement of the experimental molar volume values appeared to be higher than that of the corresponding empirical rate of change. The observed variations of both the empirical and the experimental density and molar volume values may be due to the introduced BCD which contains various positive cations, where these cations fill mostly the network vacancies, and in turn decreases the internal free volume. Accordingly the density is logically increased, while the molar volume is gradually decreased, as BCD was gradually increased.

It is worth to state that, the higher empirical density as well as the lower empirical molar volume in comparison to the corresponding experimental values can be taken also as evidences for the amorphous nature and the short range order character of the studied samples. It can be stated also that, it is possible to obtain pure glasses with higher amounts of BCD up to 60 mol%.

The frequency dependence total conductivity ($\sigma_{(\omega,T)}$) for all samples follows the exponent law of the following equation (no. 4),

$$\left(\frac{\mu}{\rho}\right)_m = \sum_i^n W_i \left(\frac{\mu}{\rho}\right)_m \quad (4)$$

where σ_{dc} is the frequency independent conductivity, A is a weakly temperature dependent factor, s is the exponent factor (usually less than unity) and ω is the angular frequency [15-17]. The obtained experimental conductivity data ($\sigma_{(T)}$) for sample no. (4) (as a representative figure), are exhibited in Figure 4 as a function of 1000/T.

It is appeared that at low temperatures the conductivity shows weak temperature dependence and strong frequency dispersion,

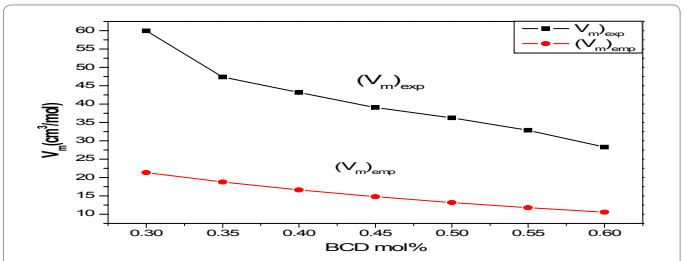

Figure 3: The variation of both the molar volume values (experimental and empirical) versus BCD content.

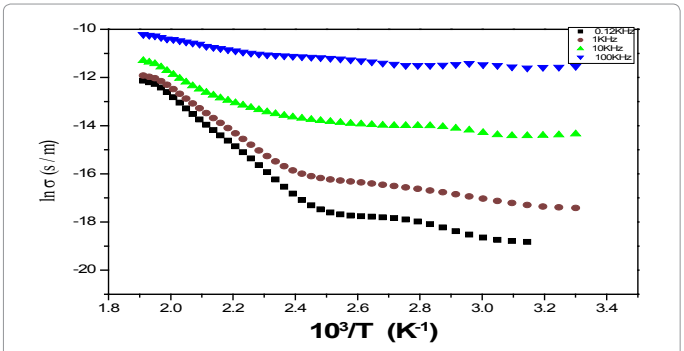

Figure 4: Total conductivity temperature dependent for sample no. (4) as representative figure.

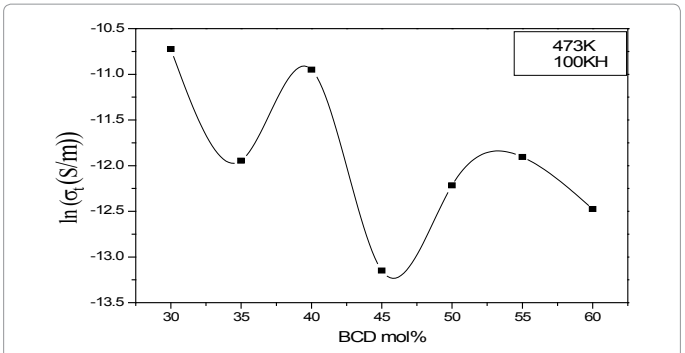

Figure 5: The total conductivity as a function of BCD content.

Sample no.	Mol.% of BCD	Mol. % of CaO	Mol.% of K_2O
1	30	18	3.36
2	35	21	3.85
3	40	24	4.4
4	45	27	4.95
5	50	30	5.5
6	55	33	6.05
7	60	36	6.6

Table 2: The concentrations of CaO and K_2O in all the prepared samples.

while at high temperatures, it shows strong temperature dependence and weak frequency dependence. It is worth to state that all sample exhibited similar behavior. It can be stated that, the dc conductivity is dominant at high temperatures while the ac conductivity is dominant at low temperatures. It is concluded also from the conductivity values that all samples behave like semiconductors [18].

Figure 5 shows the variation of $\ln\sigma_T$ as a function of BCD, where two maxima and two minima are easily observed. It is easy to observe also that, all $\ln\sigma_T$ values are fluctuated between 13 s/m and 11 s/m. Since the used BCD consists of about 60.4% CaO and 10.7% of K_2O, it is supposed that an electrical resistance appeared due to the interaction between the alkali and the alkaline earth cations at some compositions. Interesting physical effects have been previously observed in studying the behavior of glassy ionic conductors by Mansour [19].

The understanding of the microscopic transport mechanism for conduction in glass is a longstanding problem in glass science. Many glasses exhibit a roughly linear behavior with changing their chemical composition. But glasses containing two different alkali oxides represent a major exception to this trend due to the mixed alkali effect (MAE) or mixed alkali earth effect (MAEE) phenomenon [20]. For the studied glasses, the deviation from linearity may be so great that two maxima (at 40 mol% and 55 mol%) and minima (at 35 mol% and 45 mol%) occur. Moreover, the MAE was observed as a dramatic non-linear trend due to the introduction of alkali (K^+) and alkaline earth (Ca^{2+}) cations, where the resistance increased with increasing the difference between the radii of both the alkali and alkaline earth cations [20,21]. The concentrations of both CaO and K_2O in all samples were calculated and exhibited in Table 2.

At a fixed temperature (325 K), the relation between $\ln(\sigma_T)$ and $\ln(\omega)$ for sample no. (4), is exhibited in (Figure 2) as a representative figure.

The dotes and solid line represent the experimental data and theoretical fitting respectively (with any equation). It can be seen that, at low frequency the conductivity is approximately stable and

independent on frequency, while at high frequency the conductivity increased [22], According to all the obtained data, it can be stated that all samples show similar semiconducting behavior (Figure 6).

The DC conductivity values were then calculated from the fitting of the experimentally obtained σ_T data with equation no. (4) and the obtained data are then plotted in Figure 7 as a function of BCD content. It is seen that the change of σ_T is a non-linear behavior and maxima and minima are exhibited at 35 mol% and 55 mol% BCD, corresponding to CaO concentrations of 21 and 33 mol% respectively and the amounts of K_2O are also 3.3 and 6.05 mol% respectively. It can be supposed that the observed nonlinear behavior may be due to the mixed Alkali (K^+) alkaline earth (Ca^{2+}) effect.

The DC activation energy of conduction can be calculated form the slopes of the obtained straight lines of the studied sample according to Arhenius equation (equation number 5) at high temperatures, where the dc conductivity is dominant.

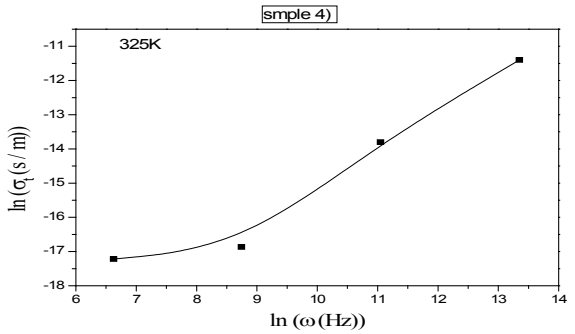

Figure 6: ln (σ_T) versus ln (ω) at a fixed temperate for the sample no. (4) as a representative curve.

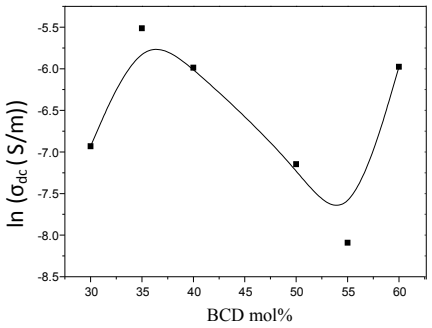

Figure 7: The DC conductivity as a function of BCD content.

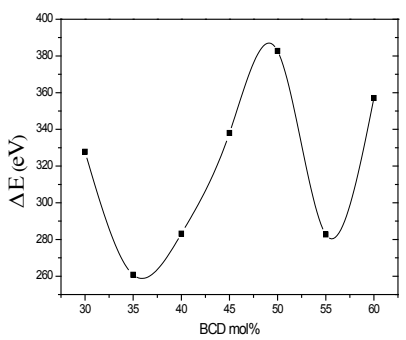

Figure 8: The DC activation energy of conduction as a function of BCD content.

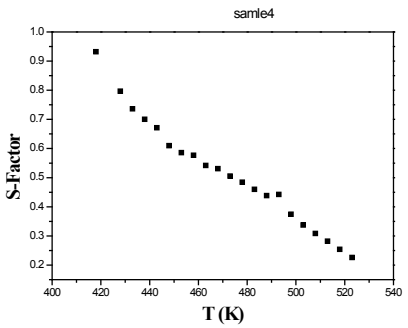

Figure 9: The variation of the S-factor as a function of temperature for sample (1) as representative figure.

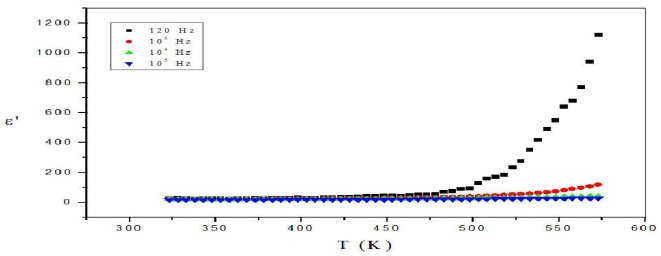

Figure 10: The di-electric constant temperature dependence at different frequencies.

$$\sigma_{dc} = \sigma_0 \exp(-\Delta E / kT) \quad (5)$$

where σ_0 is the pre-exponential factor and ΔE is the activation energy. The variation of the activation energy with BCD is exhibited in Figure 8 where this figure shows approximately the reverse behavior of the conductivity [23] and such trend was expected to be logic.

Figure 9 shows the variation of the s-factor as a function of temperature for sample no. (4), as representative figure. The obtained values of the exponent factor (s), for all samples, show approximately linear decrease with the increase of temperature. Because of the agreement between the experimental behavior of the exponent factor (S) and those predicted by the CBH model (equation (6)), proposed by Elliot [19]. It is supposed that such model can be used to describe the conduction mechanism in these glasses, and it is observed that, all samples exhibit the same behavior.

$$S = 1 - \frac{6KT}{W_m - KT\ln(\omega\tau_0)} \quad (6)$$

where ($\tau_0 = f_o^{-1}$) is the characteristic relaxation time in between 10^{-9} and 10^{-12} sec, k is the Boltzman constant, T is the absolute temperature and W_m is the energy required to remove an electron from its site to infinity.

The dielectric constant (ε') has been also measured, and Figure 10 shows the variation of ε' as a function of temperature for sample no. (4), as representative figure. It is observed that at low temperatures ε' is almost independent of temperature, while at high temperatures it increases gradually as the temperature was increased, but it shows an inverse variation with frequency. The reason for this behavior is that, the electric dipoles move almost parallel to the ac external electric field and create an inverse internal electric field. With the increase of temperature the movement of the electric dipole is easier and the dipoles move parallel to the ac external electric field and then the internal electric field increased and acts to decrease the dielectric

constant [19,23]. It is also found that all samples exhibited similar behavior.

On the other hand, Figure 11 shows the variation of the dielectric loss factor (ε″) as a function of temperature for sample no. (4) as a representative figure. It is clear that at low temperatures ε″ exhibit approximately stable value, while at high temperatures it starts to increase as the temperature was increased, and the increment rate is inversely proportional to the frequency. This behavior was explained by Stevels [24,25] who divided the relaxation phenomena into three parts, the conduction loss, the dipole loss and the vibrational loss. Since the conduction loss is proportional to σ(ω), therefore ε″ increases as the conductivity increased, where σ(ω) is temperature dependent quantity.

Until now, the majority of the nuclear radiation shields consists of layers of different concretes with different compositions and densities. But considerable variations in water contents in concretes add high uncertainty factor in calculating the attenuation coefficients and moreover, they are also opaque to visible light [26]. With the development of the X-COM computer program the mass attenuation coefficient for different shielding materials can be calculated [27,28]. Material to be used for shielding should have homogeneous density and composition. Glasses are promising materials in this regard.

The main objective is to correlate between the composition and structure of studied glasses and their attenuation behaviors to examine the suitability for users as radiation-shielding materials.

The mass attenuation coefficient is written as:

$$\mu_m = \ln(I_0 / I) / \rho x \quad (7)$$

Where ρ is the density of material (g/cm^3), I_0 and I are the incident and transmitted intensities, respectively, and x is the thickness of absorber (cm).

The Theoretical value of the total mass attenuation coefficients of mixture or compound has been calculated by WinXCom, based on the mixture rule [26].

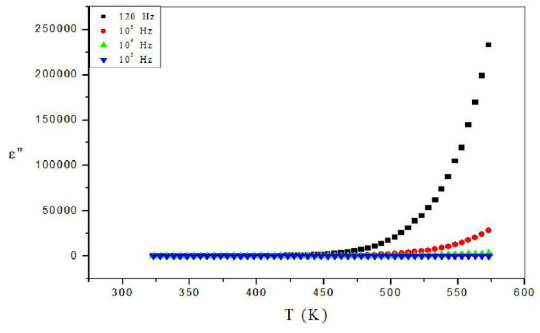

Figure 11: The variation of the dielectric loss factor (ε″) as a function of temperature.

Glass No	BCD (mol %)	Density (gm/cm^3)	μ_m (cm^2/gm) × (10^{-2})			
			356 Kev	662 Kev	1173 Kev	1332 Kev
1	30	0.8183	9.851	7.44	5.641	5.289
2	35	0.950	9.858	7.471	5.67	5.317
3	40	1.083	9.864	7.502	5.699	5.344
4	45	1.215	9.871	7.532	5.728	5.371
5	50	1.348	9.877	7.563	5.757	5.398
6	55	1.480	9.884	7.593	5.786	5.425
7	60	1.612	9.89	7.64	5.816	5.445

Table 3: The mass attenuation coefficient as a function of BCD content at relatively low γ – ray energies.

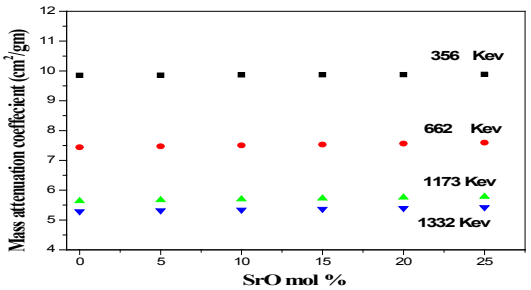

Figure 12: The mass attenuation coefficient as a function of BCD content at different γ – ray energies.

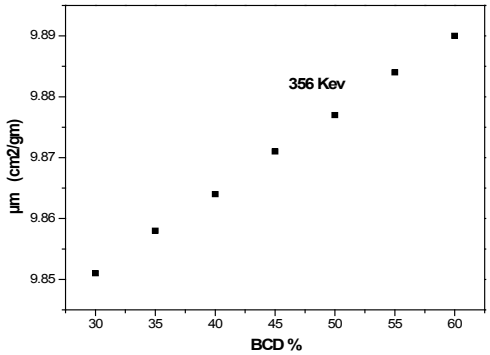

Figure 13: The mass attenuation coefficient as a function of BCD content at 356 Kev.

$$\left(\frac{\mu}{\rho}\right)_m = \sum_i^n W_i \left(\frac{\mu}{\rho}\right) \quad (8)$$

Where (μ/ρ) m is the total mass attenuation coefficient for the individual element in each component and wi is the fractional weight of the element in each component.

This mixture is valid when the effects of molecular binding, chemical and crystalline environment are negligible. Theoretical values for the total mass attenuation coefficient can be found in the tables prepared by Hubbell and Seltzer. Berger and Hubbell developed XCOM program for calculating the total mass absorption coefficients or the photon interaction cross- sections for any element, compounds or mixtures at various photon energies from (1 keV to 100 GeV). Recently, XCOM was transformed to the Windows platform by Gerward et al. [27], where it called WinXCom.

The following mass attenuation coefficient relates half value layer to linear attenuation coefficient (μ_L):

$$HVL = 0.693/\mu \quad (9)$$

where HVL is half value layer and μ_L is the linear attenuation coefficient (cm)

The obtained gamma-ray attenuation coefficient and the Half Value Layer:

Mass attenuation coefficient

Figure 12 shows the calculated results of the mass attenuation coefficients of the studied glass samples for different energies (low gamma-ray energies) as a function of BCD content; It was found that the mass attenuation coefficients (μ_m) of all samples show generally an increase only slowly with the increase of the weight fraction of BCD

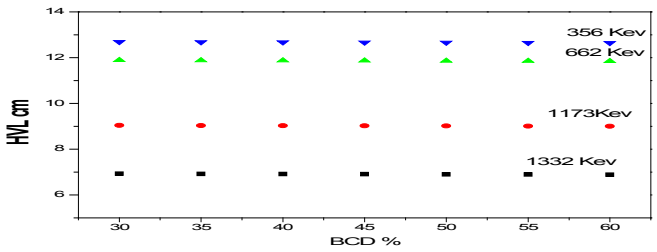

Figure 14: The half value layer as a function of BCD content at relatively low γ – ray energies.

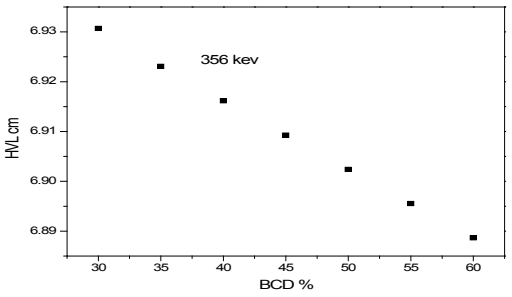

Figure 15: The half value layer as a function of BCD content at 356 Kev.

Glass No	BCD (mol %)	Density (gm/cm³)	HVL			
			356 Kev	662 Kev	1173 Kev	1332 Kev
1	30	1.92905	9.999	7.665	5.828	5.462
2	35	2.34899	10.01	7.670	5.831	5.465
3	40	2.47639	10.02	7.675	5.835	5.469
4	45	2.62365	10.03	7.681	5.838	5.472
5	50	2.70551	10.04	7.686	5.842	5.475
6	55	2.85243	10.05	7.691	5.845	5.478
7	60	3.15972	10.06	7.696	5.848	5.481

Table 4: The half value layer as a function of BCD content at relatively low gamma-ray ray energies.

at the expense of P_2O_5. This may be due to the gradual increase in the density of the investigated glass samples (Figure 13). In addition, the increase in photon interaction probability at these energies leads to the decrease the gamma-rays transmission with the increase in the amount of P_2O_5, which indicates the better shielding properties.

The numerical values of the calculated mass attenuation coefficients (μm) at different energies are summarized in Table 3.

The Half Value Layer (HVL)

HVL is the thickness of a material required to reduce the intensity of the transmitted radiation to its half value. Such value can be used to describe the effectiveness of the studied shields. Definition from the European Nuclear Society]. Figure 14 shows the behavior of the HVL for the studied glasses with different amounts of BCD and various gamma-ray energies. These figures indicate that the half value layer (HVL) decreases with the increase of the weight fractions of BCD. This may be due to the higher values of mass attenuation coefficients and the densities of the studied glass samples. The numerical values of the calculated HVL at different energies are summarized in Table 4.

Generally, these results indicate that the present glass system is a good attenuator for gamma photons (Figure 15) and promising gamma-ray shielding material due to their high mass attenuation coefficient and their low half value layer (HVL). Finally, it is worth to mention that the present glass system will open new possibility for a lead-free radiation protecting glass with non-toxicity to our environment.

Conclusion

It was found that the recycling of BCD in the glass manufacture is a matter of interest due the accumulation of huge amounts as well as its dangerous attack to the human reparatory system. It was concluded also that, phosphate glasses accept up to 60 mol% of BCD to give pure transparent and homogenous glasses, which evidenced by comparing the experimental and empirical density and molar volume values, as well as by XRD results It was found, electric transport properties studies that all glasses behave like semiconductors. The mixed alkali effect and the amount of CaO present act to corrupt the expected linear behavior of the total conductivity dependence BCD concentration.

The present glass system is a good attenuator for γ –photons and promising gamma-ray shielding material due to their high mass attenuation coefficient and their low half value layer (HVL) to certain low gamma-ray energy.

References

1. Moustafa YM, El-Adawy A (2000) Structural and physical properties of iron oxychloride phosphate glasses. Physica Status Solidi (a) 179: 83-93.
2. Metwalli E, Karabulut M, Sidebottom DL, Morsi MM, Brow RK (2004) Properties and structure of copper ultraphosphate glasses. J Non-Cryst Sollids. 344: 128-134.
3. Martin SW (1991) Ionic conduction in phosphate glasses. Am Ceram Society 74: 1767-1784.
4. Mercier R, Malugani JP, Fahys B, Robert G (1981) Superionic conduction in Li_2S-P_2S_5-LiI-glasses. Solid State Ionics 5: 663-666.
5. Wada H, Menetrier M, Levasseur A, Hagenmuller P (1983) Preparation and ionic conductivity of new B2S3-Li2S-LiI glasses. Mater Res Bull 18: 189-193.
6. Mori H, Matsuno H, Sakata H (2000) Small polaron hopping conduction in V_2O_5–Sb–TeO_2 glasses. J. Non-Cryst Solids 276: 78-94.
7. Kattak GD, Khfaja EE, Wenge LE, Thompson DJ, Said MA (1990) Non-crystalline solids. J Non-Cryst Solids 1: 194.
8. Saeed A, Elbashar YH, El-Azm AA, El-Okr MM, Comsan MN (2014) Gamma ray attenuation in a developed borate glassy system. Radiat Phys Chem 102: 167-170.
9. Saudi HA, Abd-Elalim A, Abou-Elnasr TZ (2015) Structure and physical properties study of some oxide glasses used as γ- ray shielding material. Nature and Scince p: 13-19.
10. El-Khayatt, Ali AM , Singh VP (2014) Photon attenuation coefficients of heavy-metal oxide glasses by MCNP code, XCOM program and experimental data: A comparison study. Nucl Inst Methods Phys Res (A),735: 207-212.
11. Bendary AA (2014) Ph. D. Thesis. Phys Dept. Of Faculty of Science, AL-Azhar University, Egypt.
12. Grandi S, Mustarelli P, Magistris A, Gallorini M, Rizzio E (2002) Synthesis of GeO_2-doped SiO_2 aerogels and xerogels. J. Non-Cryst Solids. 303: 208-217.
13. Feltri A, Grandi S, Mustarelli P, Cutroni M, Mandanici A (2002) GeO_2-doped silica glasses: An AC conductivity study. J. Solid State Ionics.154: 217-21.
14. Duhan S, Sanghi S, Agarwal A, Sheoran A, Rani S (2009) Dielectric properties and conductivity enhancement on heat treatment of bismuth silicate glasses containing TiO_2. Physica B: Condensed Matter. 404: 1648-1654.
15. Takada T, Wang SF, Yoshikawa S, Jang SJ, Newnham RE (1994) Effect of glass additions on BaO–TiO_2–WO_3 microwave ceramics. J Am Ceram Soc 77: 1909-1916.
16. Wu S, Wei X, Wang X, Yang H, Gao S (2010) Effect of Bi_2O_3 additive on the microstructure and dielectric properties of $BaTiO_3$-based ceramics sintered at lower temperature. J Mater Sci Technol 26: 472-476.
17. Muralidharan P, Venkateswarlu M, Satyanarayana N (2005) Acid catalyst

concentration effect on structure and ion relaxation studies of Li_2O–P_2O_5–B_2O_3–SiO_2 glasses synthesized by sol–gel process. J Non-Cryst Solids 351: 583-594.

18. Abdel-Ghany AM, Bendary AA, Abou-El-Nasr TZ, Hassaan MY, Mostafa AG (2014) Electrical transport properties of some sodium silicate glasses containing by-pass cement dust. Nature and Science 12: 6.
19. Fowler TG, Elliott SR (1987) Continuous random network models for a-As_2S_3. Journal of non-crystalline solids. 92: 31-50.
20. Fouad SS, Bekheet AE, Farid AM (2002) Derivation of a relation between the conduction mechanism and chemical bonding of amorphous Ge 15 Se 85−x Agx alloys. Physica B: Condensed Matter. 322: 163-172.
21. Abdel-Ghany AM (2011) Ph. D. Thesis, Phys. Dept of Faculty of science AL-Azhar Univ,Egypt.
22. Jayasinghe GD, Dissanayake MA, Bandaranayake PW, Souquet JL, Foscallo D (1999) Electronic to ionic conductivity of glasses in the Li_2O–V_2O_5–TeO_2 system. Solid State Ionics. 121: 19-23.
23. Fouad SS, Bekheet AE, Farid AM (2002) Derivation of a relation between the conduction mechanism and chemical bonding of amorphous Ge 15 Se 85−x Agx alloys. Physica B: Condensed Matter 322: 163-172.
24. Efimov AM (1997) IR fundamental spectra and structure of pyrophosphate glasses along the $2ZnO\cdot P_2O_5$–$2Me_2O\cdot P_2O_5$ join (Me being Na and Li). J Non-cryst Solids 209: 209-226.
25. Eldin FE, El-Alaily NA (1998) Electrical conductivity of some alkali silicate glasses. Materials Chem and Phys 52: 175-179.
26. Krocher JF, Browman RE (1984) Effects of radiation on materials and components. Reinhold, New York.
27. Gerward L, Guilbert N, Jensen KB, Levring H (2001) X-ray absorption in matter. Reengineering XCOM, Radiat Phys Chem 60: 23-24.
28. Abdel-Ghany AM, Zoulfakar AM (2015) Blast furnace slag as a raw material to manufacture gamma-ray transparent shield glass. American Journal of Phys and Applications. 3: 208-214.